LA-UR 91-3455

LA-UR--91-3455

DE92 002520

Los Alamos National Laboratory is operated by the University of California for the United States Department of Energy under contract W-7405-ENG-36.

TITLE: STATE DENSITIES WITH LINEAR MOMENTUM AND THEIR APPLICATION TO PREEQUILIBRIUM AND PHOTOABSORPTION REACTIONS

AUTHOR(S): M. B. Chadwick, T-2
P. Oblozinsky, Inst. of Physics, Slovak Academy of Sciences, Bratislava, Czechoslovakia

SUBMITTED TO: Presentation at the Technical University Dresden for the International Symposium on Nuclear Physics, Dresden (Gaussig), Germany, 9-12 Nov. 1991.

DISCLAIMER

Los Alamos
Los Alamos National Laboratory
Los Alamos, New Mexico 87545

State densities with linear momentum and their application to preequilibrium and photoabsorption reactions

M.B. Chadwick
Theoretical Division, Los Alamos National Laboratory, Los Alamos, New Mexico 87545

P. Obložinský
Institute of Physics, Slovak Academy of Sciences, 842 28 Bratislava, Czechoslovakia

We discuss the concept of state densities with linear momentum and describe their application to preequilibrium reaction theory as well as nuclear photoabsorption via the quasideuteron mechanism. An exciton model is presented for particle emission in nucleon-induced reactions in which linear momentum conservation is included. The nucleon emission contributions from the first two preequilibrium stages are calculated by determining exact particle-hole state densities with a specific energy and linear momentum in a Fermi-gas model of the nucleus. Angular distributions arise naturally from our treatment and do not have to be added in an *ad hoc* way. The angular distributions that we obtain from the first two preequilibrium stages are identical to those found using the Kikuchi-Kawai quasifree scattering kernel. Since many preequilibrium analyses are based upon an equidistant single-particle model of the nucleus, we also determine the state densities with linear momentum (and hence angular distributions) in such a model. A no-parameter quasideuteron model of photoabsorption is presented in which the Levinger parameter and Pauli-blocking function are determined theoretically, using state densities with linear momentum. Comparisons with data are shown, and the temperature dependence of the photoabsorption cross section is calculated.

I. INTRODUCTION

All theoretical descriptions of nuclear reactions in the continuum region make statistical assumptions concerning the complex multistep reaction process. In order to calculate cross sections for preequilibrium emission one simplifies the complicated nature of the different possible scattering processes by introducing averaged matrix elements of the various possible transitions and state densities for the different particle-hole preequilibrium configurations. Expressions for the state densities represent an integral part of any theoretical calculation, and a number of different approaches for obtaining such densities have been developed. Frequently an equidistant single-particle-state model is adopted, allowing a simple evaluation of the particle-hole state density. If there are no restrictions on the particle-hole excitations the formulae of Ericson [1] and Williams [2] result. Including finite well-depth restrictions leads to the slightly more complicated expressions in [3]. Partial state densities within an equidistant single particle model have been developed to describe the angular momentum [2], parity [4], and isospin [5] structure of the states. We have recently extended such ideas to obtain the linear-momentum structure of such particle-hole state densities [?,6].

The linear momentum structure of a state density is a useful concept since, for reasonably high excitation energies, a semiclassical description of the nucleus (where one pictures the individual nucleon states as eigenstates of linear momentum) becomes more realistic. By considering the variation of the accessible residual nucleus state density with nucleon emission angle, it is possible to obtain angular distributions of emitted particles in a consistent manner. We also describe how state densities with linear momentum can be used in a quasideuteron model of photoabsorption. We found such densities essential for a realistic description of the correlated nature of neutron-proton emission in photoabsorption processes above the giant resonance and below the pion threshold.

In section II we discuss state densities with linear momentum, and how they can be calculated both for a Fermi-gas and an equidistant single-particle-state model. In section III we describe two different applications of state densities with linear momentum. Section IIIA descibes how angular distributions can be obtained in an exciton model of preequilibrium reactions, and an account of this work is to appear in the November 1991 issue of Physical Review C - Rapid Communications. Section IIIB gives a description of out quasideuteron photoabsorption model (full details can be found in Ref.[?]) and we give some conclusions in section IV.

II. STATE DENSITIES WITH LINEAR MOMENTUM

We shall now show how state densities with linear momentum are calculated. We view the nucleus semiclassically, and wish to determine the number of $p-h$ states with an energy in the range $E \rightarrow E+dE$ and a total momentum in the range $\mathbf{K} \rightarrow \mathbf{K}+d^3\mathbf{K}$. This problem was first investigated by Madler and Reif [?] who used a partition-function approach. Unfortunately, their method is valid only for large numbers of excited particles and holes, and for most applications in nuclear reaction theories it is the simple particle-hole excitations that are most important. In addition, their approach suffers from some computational difficulties in making saddle-point approximations. Maddler and Reif's approach has been extended by Iwamoto [?] for use in heavy-ion calculations. Our approach, on the otherhand, is exact and leads to simple analytic expressions for the simplest $p-h$ state densities. The more complicated $p-h$ densities become harder to solve using our method due to the high-dimensionality of the integrations, though for many applications (including those shown in this paper) it is only densities for simple $p-h$ excitations that are needed.

In order to make our approach more transparent, we first indicate how state densities without linear momentum can be determined. The state density of a p-particle h-hole system can be obtained by convoluting single-particle and -hole densities with an energy-conserving delta-function. When linear momentum effects are not accounted for, this can be expressed as

$$\rho(p,h,E) = \frac{1}{p!h!}\int_{i=1}\cdots\int_{i=p}\int_{j=1}\cdots\int_{j=h}\delta(E-\sum_{i=1}^{p}\epsilon_i+\sum_{j=1}^{h}\epsilon_j)$$

$$\times\prod_{i=1}^{p}\rho(1p,\epsilon_i)\;\theta(\epsilon_i-\epsilon_{_F})\;d\epsilon_i\;\prod_{j=1}^{h}\rho(1h,\epsilon_j)\;\theta(\epsilon_{_F}-\epsilon_j)\;d\epsilon_j, \qquad (1)$$

where i labels the particles and j the holes. The theta functions are unity if their argument is greater than zero and zero otherwise, accounting for Pauli-blocking. The densities of single-particles and -holes in energy space are represented by $\rho(1p,\epsilon_i)$ and $\rho(1h,\epsilon_j)$, with the energies $\epsilon_{i,j}$ measured relative to the bottom of the nuclear well. The factorials $p!$ and $h!$ account for the indistinguishability of the particles and holes. If an equidistant single-particle model of the nucleus is used, the above expression would yield the Ericson state density expression, corrected to include finite nuclear well depth restrictions [?]. In a Fermi-gas model of the nucleus the single-particle and -hole densities in energy space are given by $\rho(1p,\epsilon_i)=3A\sqrt{\epsilon_i}/2\epsilon_{_F}^{3/2}$ and $\rho(1h,\epsilon_j)=3A\sqrt{\epsilon_j}/2\epsilon_{_F}^{3/2}$, where A is the nuclear mass number.

We now generalize the above expression to allow state densities with a specific linear momentum to be determined. The convolution of the single-particle and -hole states is now performed in momentum space, and a linear-momentum conserving delta function is included in the integration,

$$\rho(p,h,E,\mathbf{K}) = \frac{1}{p!h!}\int_{i=1}\cdots\int_{i=p}\int_{j=1}\cdots\int_{j=h}\ \delta(E-\sum_{i=1}^{p}\epsilon_i+\sum_{j=1}^{h}\epsilon_j)$$

$$\times\delta(\mathbf{K}-\sum_{i=1}^{p}\mathbf{k}_i+\sum_{j=1}^{h}\mathbf{k}_j)\ \prod_{i=1}^{p}\rho(1p,\mathbf{k}_i)\ \theta(k_i-k_F)\ d^3\mathbf{k}_i\ \prod_{j=1}^{h}\rho(1h,\mathbf{k}_j)\ \theta(k_F-k_j)\ d^3\mathbf{k}_j, \tag{2}$$

where $\mathbf{k}_i$ and $\mathbf{k}_j$ are the single-particle and -hole linear momenta, and k_F is the Fermi momentum. The density of single-particle and -hole states in momentum space are $\rho(1p,\mathbf{k}_i)$ and $\rho(1h,\mathbf{k}_j)$ respectively.

Neither Eq. (1) nor Eq. (2) include the possibility that some of the excited particles/holes can Pauli-block other particles/holes, though for the simple particle-hole configurations that we consider this effect can be safely ignored. As expected from symmetry, the density of states with linear momentum, $\rho(p,h,E,\mathbf{K})$, is independent of the direction of the total momentum $\mathbf{K}$ and depends only upon its magnitude. The dimensions of the state densities with linear momentum are $\mathrm{MeV}^{-1}(\mathrm{MeV/c})^{-3}$, and they obey the relation

$$\rho(p,h,E) = \int \rho(p,h,E,\mathbf{K})\ 4\pi K^2 dK. \tag{3}$$

This equation also allows a useful check on analytic expressions that are derived for state densities with linear momenta. If they are integrated over all values of total momenta they must yield the 'conventional' state densities, which are only a function of energy.

A. The Fermi-gas model

In the Fermi-gas model the single-particle and -hole states are eigenstates of linear momentum, the density of such states in momentum-space being a constant which reproduces the number of nucleons,

$$\rho(1p,\mathbf{k}_i) = \rho(1h,\mathbf{k}_j) = \frac{A}{\frac{4}{3}\pi k_F^3} \equiv \kappa. \tag{4}$$

Below we give some analytic results for state densities with linear momentum for $p-h$ configurations which are important in preequilibrium reactions and will be used in the next section. We shall consider particle emission from only the first two preequilibrium stages since these dominate the preequilibrium spectrum for most nucleon-induced reactions. Thus we must evaluate the state densities for $1p1h$, $2p1h$, $2p2h$ and $3p2h$ excitations. The $\rho(1p,1h,E,\mathbf{K})$ density requires the solution of a six-dimensional integration, which can be solved analytically using the techniques shown in Ref. [7], giving

$$\rho(1p,1h,E,\mathbf{K}) = \frac{\pi m K^2}{K} \times \begin{cases} \left[k_F^2 - \left(\frac{mE}{K} - \frac{K}{2}\right)^2\right] & \text{if } K_{\min} < K < K_1 \text{ or } K_2 < K < K_{\max} \\ 2mE & \text{if } K_1 < K < K_2 \\ 0 & \text{otherwise.} \end{cases} \tag{5}$$

where

$$K_{\substack{\min \\ \max}} = \sqrt{2mE + k_F^2} \mp k_F, \tag{6}$$

$$K_{\substack{1 \\ 2}} = \sqrt{2(k_F^2 - mE) \mp 2k_F\sqrt{k_F^2 - 2mE}}. \tag{7}$$

The high-dimensionality of the integrations for the evaluation of the more complex state densities can be reduced by breaking up the integrals, making use of analytic solutions for simpler configurations. For instance, the $\rho(2p,2h,E,\mathbf{K})$ requires a twelve-dimensional integration, though it can be expressed as a convolution of two $1p1h$ state densities, each of which is known analytically, so that

$$\rho(2p,2h,E,\mathbf{K}) = \frac{1}{2!\,2!}\int\int \rho(1p,1h,E_1,\mathbf{K}_1)\;\rho(1p,1h,E-E_1,\mathbf{K}-\mathbf{K}_1)\;d^3\mathbf{K}_1\;dE_1, \tag{8}$$

which, by symmetry, can be reduced to a three-dimensional integral and can be solved numerically without any difficulties. We checked that when the state densities with linear momentum are integrated over all total momenta [using Eq. (3)] they yield the Fermi-gas state densities without linear momentum of Eq. (1).

In Fig. 1 the variation of the residual nucleus $1p1h$ and $2p2h$ state densities [Eqs. (5) and (8)] with emission angle is shown for the reaction ^{184}W(n,n') for an incident energy of 26 MeV and emission energies of 14.5 and 18.5 MeV. A Fermi energy of 35 MeV was adopted. These densities are strongly forward-peaked due to the variation of the state density with the linear momentum deposited in the residual nucleus. This forward peaking decreases with increasing exciton number as the linear momentum brought in by the projectile is shared among more particles and holes and the memory of the incident direction is lost. Since the angular distribution of emitted particles comes from the variation of the residual-nucleus phase space with emission angle, no preequilibrium emission from the $n = 3$ stage can occur for angles greater than about 110 degrees. This is a kinematical effect resulting from the restrictions of energy and momentum conservation and is also seen in Refs. [8, 10].

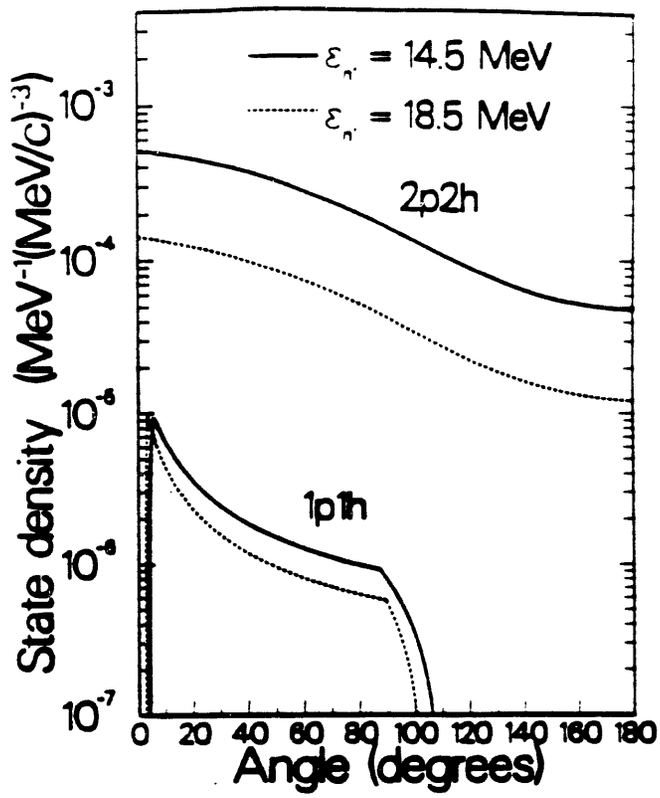

FIG. 1. The variation of the 1p1h and 2p2h state densities with emission angle for the residual nucleus in the reaction ^{184}W(n,n'). The incident energy is 26 MeV, and the emission energies are $\epsilon_{n'}$=14.5 and 18.5 MeV.

FIG. 1. The variation of the $1p1h$ and $2p2h$ state densities with emission angle for the residual nucleus in the reaction ^{184}W(n,n'), using a Fermi-gas model. The incident energy is 26 MeV, and the emission energies are $\epsilon_{n'}$=14.5 and 18.5 MeV.

B. Equidistant single-particle-state model

The above subsection contained expressions for state densities with linear momentum in a Fermi gas model of the nucleus. In such a model the single-particle states in energy space increase as the square-root of the excitation energy, and are constants in momentum space. In this section we shall indicate how state densities with linear momentum can be obtained for equidistant single-particle levels in energy space. This is of importance since preequilibrium reaction theories almost always use state densities which are based upon equidistant single-particle levels, duc to their computational simplicity.

The particle-hole state density is determined using Eq. (2). We need, however, to determine the single-particle density in momentum space which yields equidistant levels in energy space. The number of single-particle states in momentum space with absolute momenta between k and $k+dk$ is

$$dN(k) = 4\pi k^2\, dk\, \rho_1(\mathbf{k}), \tag{9}$$

where $\rho_1(\mathbf{k})$ denotes either $\rho(1p, \mathbf{k}_i)$ or $\rho(1h, \mathbf{k}_j)$, the single-particle (and -hole) density that we are determining. For equidistant levels in energy space, $dN(\epsilon) = g\, d\epsilon$, ϵ being the excitation energy and g the constant single-particle density. Since $\epsilon = k^2/2m$, this equation can be expressed as

$$dN(k) = \frac{gk}{m}\, dk. \tag{10}$$

Equations (??) yield the result for the single-particle density in momentum space,

$$\rho(1p, \mathbf{k}_i) = \rho(1h, \mathbf{k}_j) = \frac{g}{4\pi m k}. \tag{11}$$

In other words, the density of single-particle states in momentum space that yields equidistant states in energy space varies as $1/k$. Since the $1p1h$ state density determines the angular distribution from single-step scattering, we show below the $1p1h$ state density with linear momentum for an equidistant single-particle level nucleus, obtained by solving the six-dimensional integral (2) with Eq. (11),

$$\rho(1p, 1h, E, \mathbf{K}) = \frac{g^2}{8\pi m K} \ln \left[\frac{k_F + \sqrt{k_F^2 + 2mE}}{k' + \sqrt{k'^2 + 2mE}} \right] \tag{12}$$

where

$$\begin{aligned} k' &= \left| \frac{mE}{K} - \frac{K}{2} \right| \quad \text{if} \quad K_{\min} < K < K_1 \quad \text{or} \quad K_2 < K < K_{\max} \\ k' &= \sqrt{k_F^2 - 2mE} \quad \text{if} \quad K_1 < K < K_2 \\ \text{and } \rho(1p, 1h, E, K) &= 0 \qquad\qquad \text{otherwise,} \end{aligned} \tag{13}$$

$K_{\min}, K_{\max}, K_1, K_2$ being given by Eqs. (6,7). As in the Fermi gas model, we again find an expression for the $1p1h$ density which has three different regions. The values of $K_{\min}, K_{\max}, K_1, K_2$ which define the boundaries of these regions are not sensitive to the particular single-particle densities adopted and are therefore identical for the Fermi-gas and equidistant models. Equation (3) must hold, indicating that if the above $1p1h$ state density is integrated over all momenta the Ericson density, with finite well-depth restrictions, results. We have checked that our Eq. (13) satisfies

$$\int \rho(1p, 1h, E, \mathbf{K}) 4\pi K^2 dK = \rho(1p, 1h, E) \equiv g^2 \left[E - (E - \epsilon_F)\theta(E - \epsilon_F) \right]. \tag{14}$$

Equation ([?]) can be compared with the analogous expression ([?]) for a Fermi-gas nucleus. While the functional form is clearly different, there are some close similarities. The angular distribution for a given emission energy arises from the dependence of the $1p1h$ state density on the momentum K, and it is seen that in the region $K_1 < K < K_2$ both Eqs. (5) and (13) show identical $1/K$ dependences.

The constant density of single-particle states in energy space is often taken as $g = A/14$, a value established from extensive data on slow neutron resonances. However, the Fermi-gas model as described in the previous section yields a density of states at the Fermi level of $3A/2\epsilon_F$, which for $\epsilon_F = 35$ MeV is a factor of 1.66 too small. This is a well known problem with the Fermi-gas model. On the otherhand, a value of $g = A/14$, while describing the density of states at the Fermi surface fairly well, overpredicts the number of nucleons by a factor of 2.5 in an equidistant model[?]. In order for a comparison to be made between the equidistant and Fermi-gas state densities, we have chosen a value of $g = 3A/2\epsilon_F$ so that the densities at the Fermi-level agree. This choice was motivated by the fact that for small excitation energies most excited particles and holes are close to the Fermi-level. In Fig. 2 the variation of the residual nucleus $1p1h$ state densities with emission angle is shown for the reaction $^{184}W(n,n')$ for an incident energy of 26 MeV and an emission energy of 18.5 MeV, for Fermi-gas and equidistant models. It is seen that the $1p1h$ state densities are very similar in the two models.

We again stress that our choice above for g was made solely to allow a comparison with our previous results for a Fermi-gas nucleus. Another approach might have been to use the commonly adopted value of $g = A/14$ for the equidistant model, but then use a Fermi-energy of 21 MeV in the Fermi-gas model in section IIa so that both models yield identical single-particle densities at the Fermi-level.

It is worth mentioning that Madler and Reif's method for determining state densities with linear momentum (which also uses an equidistant single-particle level model) fails completely for the important $1p1h$ state density with linear momentum. They show in Fig. 2 of Ref. [?] the variation of their $1p1h$ density with emission angle, which differs considerably in shape from our exact result in our Fig. 2. The shape of the $1p1h$ density is critically important in determining the angular distribution of emitted particles.

FIG. 2 the variation of the residual nucleus $1p1h$ state densities with emission angle, for the reaction $^{184}W(n,n')$ for an incident energy of 26 MeV and an emission energy of 18.5 MeV, for Fermi-gas and equidistant models.

III. APPLICATIONS OF STATE DENSITIES WITH LINEAR MOMENTUM

A. Angular distributions in the exciton preequilibrium model

It has been established that non-equilibrium processes play an important role in nuclear reactions induced by light projectiles with incident energies above about 10 MeV. The characteristic features of particle emission from the composite nucleus before equilibrium has been reached (preequilibrium emission) are an excess of high-energy particles, and a forward peaking in the observed angular distributions. The overabundance of high-energy particles is due to the nuclear excitation energy being shared among only a few degrees of freedom in the early stages of the reaction when preequilibrium emission occurs, and the forward peaking is indicative of the incident projectile's direction being partially preserved. Both quantum mechanical and semi-classical theories have been developed to account for preequilibrium emission. Quantum mechanical approaches such as that of Feshbach, Kerman, and Koonin (FKK) [12], Tamura *et al.* [13] and Koning and Akkermans [?] have been able to successfully describe the spectral shape and angular distribution of emitted particles, though the calculations are rather involved and their predictive power is limited [15]. The semiclassical exciton [16] and hybrid [17] preequilibrium models, on the other hand, are able to describe the angle-integrated spectral shapes successfully, though in their usual formulation they cannot yield angular distributions directly. In this section we shall show that by modifying the exciton model to include linear momentum effects it yields angular distributions in a natural and consistent way. We shall not explicitly discuss the hybrid model, though the modifications needed in it for the inclusion of linear momentum effects should be similar to those that we present for the exciton model.

In the exciton model the particle emission rates from the preequilibrium stages of the reaction are calculated by invoking microscopic reversibility and applying phase-space arguments. In its usual formulation it does not conserve linear momentum in the various intra-nuclear transitions and can not yield information concerning the angular distribution of emitted particles. In order to obtain such information, it has become commonplace to include in the model, in an *ad hoc* manner, a nucleon-nucleon scattering kernel obtained either from free nucleon-nucleon scattering [18, 19] or, more realistically, from quasifree scattering in nuclear matter using the Kikuchi-Kawai (KK) expression [10, 20–23], for reviews see Refs. [24, 25]. While the inclusion of a nucleon-nucleon scattering kernel within an exciton model is a physically plausible way to obtain angular distributions, no formal theoretical connection has been made between the exciton model and quasifree scattering descriptions. We shall show that by conserving linear momentum in the exciton model and by using the Fermi-gas

state densities with linear momentum described in the previous section, the angular distributions obtained are identical to those found using KK quasifree scattering. We do not make use of the *fast particle* approximation, as in Ref. [18], but treat the excited particles and holes for a given preequilibrium stage statistically. The forward-peaked angular distributions that we obtain arise purely from phase-space factors, and possible dynamical effects are disregarded.

In the previous section we presented a method for exactly determining state densities with linear momentum. Since our approach involves convoluting single-particle and -hole states in a Fermi-gas nucleus, the complexity of the integrals increases rapidly for more complex preequilibrium stages. We are able, however, to determine the state densities with linear momentum needed for the calculation of first and second stage preequilibrium emission in nucleon-induced reactions. We assume, following Chiang and Hüfner [26], that preequilibrium emission beyond the second stage can be ignored before equilibrium emission occurs.

In the exciton model it is assumed that an incident nucleon interacts with the target nucleus to form a two-particle-one-hole ($2p1h$) state, and in subsequent two-body nucleon-nucleon interactions the excited system may pass through more complex particle-hole configurations towards equilibrium. Particle emission can occur from the early preequilibrium stages and these particles typically contribute to the high-energy part of the emission spectrum. The double-differential cross section for the emission of a particle with energy ϵ and direction Ω can be written as

$$\frac{d^2\sigma}{d\epsilon d\Omega} = \sigma_R \sum_{\substack{\Delta n=+2 \\ n=3}} \frac{\lambda_n(\epsilon,\Omega)}{\Lambda_n^+ + \Lambda_n} D_n, \tag{15}$$

where the number of excitons is $n = p + h$. The reaction cross section of the incident particle on the target nucleus is σ_R, and D_n is the depletion factor, representing the probability that the system reaches the n-exciton configuration without preequilibrium decay. Λ_n^+ and Λ_n are the total rates for decay to more complex exciton configurations and for particle emission, respectively, and $\lambda_n(\epsilon,\Omega)$ is the double-differential emission rate for a given type of particle. This is found from microscopic reversibility to be

$$\lambda_n(\epsilon,\Omega) = \frac{m\epsilon\,\sigma_{\rm inv}(\epsilon)R(p)}{2\pi^3\hbar^3}\,\frac{\rho(p-1,h,E-\epsilon_\Omega,\mathbf{K}-\mathbf{k}_\Omega)}{\rho(p,h,E,\mathbf{K})}, \tag{16}$$

where the reaction cross section for the inverse process of nucleon absorption on the residual nucleus is $\sigma_{\rm inv}(\epsilon)$. The composite system total energy and momentum before particle emission are E and $\mathbf{K}$ respectively, and the residual nucleus energy and momentum after emission are $E - \epsilon_\Omega$ and $\mathbf{K} - \mathbf{k}_\Omega$ respectively, all these quantities being measured relative to the bottom of the nuclear well. The energy and momentum of the emitted particle relative to the bottom of the nuclear well are $\epsilon_\Omega = \epsilon + B + \epsilon_F$ and $\mathbf{k}_\Omega$, where $|\mathbf{k}_\Omega| = \sqrt{2m(\epsilon + B + \epsilon_F)}$, B being the binding energy and ϵ_F the Fermi

energy. $R(p)$ is a correction factor to account for neutron-proton distinguishability, and is discussed below. In the above expression state densities with linear momentum are shown, though the state densities that are used in the original exciton model are a function of energy only.

From Eq. (16) it is clear that the angular distribution of emitted particles from a preequilibrium stage arises from phase-space factors. For a given particle emission energy, the various emission directions result in different total momenta being transfered to the residual nucleus, with corresponding different accessible state densities. Thus the angular distribution of emitted particles from the $n = 3$ stage (i.e. single-step scattering) is given by the variation of $\rho(1p, 1h, E - \epsilon_\Omega, \mathbf{K} - \mathbf{k}_\Omega)$ with the emission angle. The angular distribution that we obtain using $1p1h$ state densities according to Eq. (5) is identical to that found by KK [10] for single-step quasifree scattering from a non-interacting Fermi-gas nucleus. An inspection of the physics involved suggests that this result is to be expected since our exciton model, and the quasifree scattering model of KK, both conserve linear momentum and energy in a Fermi-gas nucleus. Furthermore, the expression used by KK for single-step scattering uses a basic free-space nucleon-nucleon cross section which is isotropic, so that all the angular dependence arises implicitly from phase space factors, as done explicitly in our approach. The similarity of our exciton model with KK's approach can be most clearly seen in the work of Chiang and Hüfner [26], who use the KK scattering function to calculate single- and double-step quasifree scattering. Their expressions for the single- and double-step scattering use nuclear response functions [27] for a non-interacting Fermi-gas, which are directly proportional to our $1p1h$ and $2p2h$ state densities with linear momentum. It should be noted that from Eq. (8) it is clear that our model yields a convolution structure for the two-step scattering, which is common to most semiclassical scattering theories as well as the quantum mechanical FKK multistep direct theory.

For the calculation of nucleon emission cross sections we used Kalbach's parametrization [28] for the transition rates to more complex configurations, Λ_n^+, which was originally determined without linear momentum considerations. This is reasonable since we found that Λ_n, obtained by integrating Eq. (16) over all angles and energies for neutrons and protons, agreed to within 5% with the value obtained when linear momentum effects were not included. Also, this integral did not differ significantly from its value obtained using the traditional Ericson equidistant single-particle level state densities, corrected for a finite nuclear well depth. The neutron-proton distinguishability factor $R(p)$ [29] in Eq. (16) is consistent with the above parametrization [*]. The reaction cross sections in Eqs. (15,16) were determined using the Becchetti-Greenlees optical potential [30], and we took the Fermi energy to be 35 MeV.

Angular distributions for 14.5 and 18.5 MeV neutrons emitted in the reaction $^{184}W(n,n')$, induced by 26 MeV neutrons. At these emission energies the equilibrium emission contributions were found to be negligible. Shown for comparison are quantum mechanical FKK calculations and experimental data, taken from Marcinkowski *et al.* [15].

We have determined angular distributions for 14.5 and 18.5 MeV emitted neutrons in the reaction $^{184}W(n,n')$ induced by 26 MeV neutrons. Our results are shown in Fig. 12 and it is evident that the observed forward peaking in the data is accounted for in our model, though we underpredict the data at backward angles. Neutron emission from the $n = 3$ stage dominates scattering in the forward direction but does not contribute beyond 110 degrees, whereas $n = 5$ emission covers all directions but is too weak to account for the backward-angle data. This underprediction was also seen in Refs. [20–22] where the KK quasifree scattering kernel was used in semiclassical preequilibrium models, and results from the absence in our model of effects such as diffraction of the nucleons in the mean-field nuclear potential [21, 22]. It is beyond the scope of the present work to include such effects, which really require a quantum mechanical treatment. The dashed line shows a quantum mechanical calculation of the neutron scattering cross section using the FKK theory [15] which uses the distorted-wave Born expansion, and with single and double-step scattering the theory describes the angular distributions well. In Fig. 13 we show the proton emission spectra at five different angles for the reaction $^{54}Fe(p,p')$ induced by 62 MeV protons. For low emission energies we have included the equilibrium emission contribution (reduced due to the reaction flux lost through $n = 3$ and $n = 5$ preequilibrium emission), determined with the Hauser-Feshbach code GNASH [32]. The shapes of the spectra generally agree fairly well with experiment, but again we underpredict the backward-angle data. We also determined the angle-integrated spectrum and found that it describes the data well (since the backward-angle cross section is a minor fraction of the total preequilibrium cross section), and have compared it with an exciton model calculation using Fermi-gas state densities which do not include linear momentum, from Eq. (1). We found differences of less than 5% , indicating that it is not necessary to include linear momentum effects when determining angle-integrated spectra.

Spectra of protons emitted at a number of angles in the $^{54}Fe(p,p')$ reaction induced by 62 MeV protons, compared with experimental data [31]. The full line shows the sum of $n = 3$ and $n = 5$ preequilibrium emission in our model, and the dash-dot line includes the equilibrium emission contribution.

The above results show that if a Fermi-gas model is used to evaluate state densities with linear momentum in an exciton model, angular distributions are obtained which are identical to those found using the KK scattering kernel. Therefore, if one used a preequilibrium model with Fermi-gas state densities which are only a function of energy (and not momentum), and in addition used a KK scattering kernel to obtain angular distributions, one would obtain identical results to those found using our above model. However, a number of authors [?,?] have adopted an inconsistent approach of using an equidistant single-particle-state model to determine state densities, with a KK scattering kernel for the angular distributions. A consistent approach would be to use the formalism shown in this section with the state densities with linear momentum from Section IIB/ Or, alternatively, use a preequilibrium model based on equidistant single-particle-states (without linear momentum considerations), in conjuction with a scattering kernel obtained from Eq. (13). Due to the close similarity between the $1p1h$ Fermi-gas and equidistant single-particle state densities seen in Fig. 2, the scattering kernel from Eq. (13) would be almost identical to that of KK.

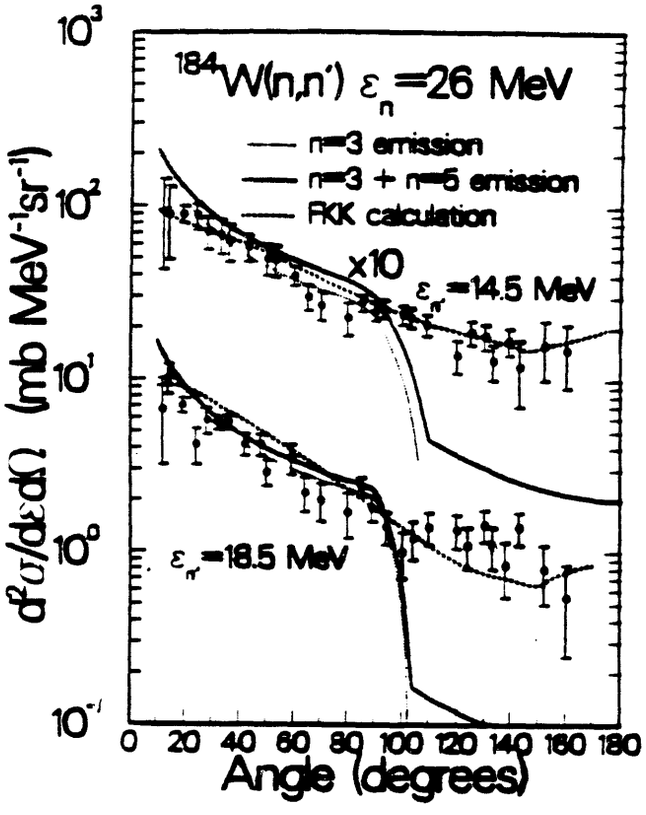

Fig 2.

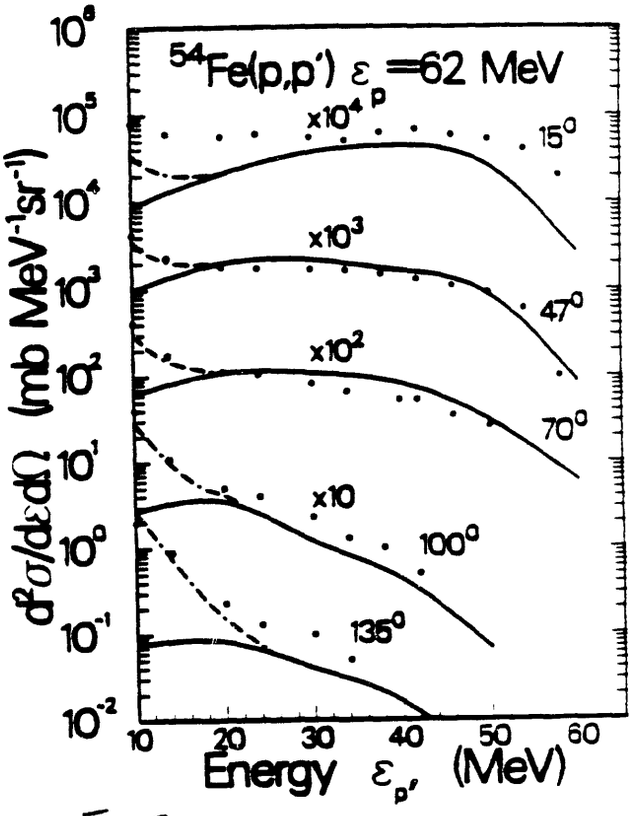

Fig 3.

B. THE QUASIDEUTERON MODEL OF NUCLEAR PHOTOABSORPTION

In this section we shall discuss another application of state densities with linear momentum: nuclear photoabsorption on correlated neutron-proton pairs via the quasideuteron mechanism. A full discussion of this application can be found in our paper [?].

The quasideuteron model describes the dominant mechanism for nuclear photoabsorption for incident photon energies in the range 40 MeV $\lesssim\epsilon_\gamma\lesssim$140 MeV. This model was first proposed by Levinger [33–35] and has subsequently been applied extensively to analyze nuclear photoabsorption cross sections [36–39]. The model does, however, contain two free parameters and treats the effects of the Pauli exclusion principle in an entirely phenomenological manner. Here we present a quasideuteron model of photoabsorption which includes Pauli-blocking effects theoretically and does not contain any free parameters. In the quasideuteron model it is assumed that photoabsorption takes place on correlated neutron-proton pairs within a nucleus. The relatively small photon wavelengths ensure that the interaction takes place with a nucleon-nucleon pair, rather than with the nucleus as a whole, and the predominantly electric-dipole nature of the interaction implies photoabsorption only by neutron-proton pairs. Levinger showed [33, 35] that the nuclear photoabsorption cross section $\sigma_{qd}(\epsilon_\gamma)$ can be expressed in terms of the free deuteron photo-disintegration cross section $\sigma_d(\epsilon_\gamma)$,

$$\sigma_{qd}(\epsilon_\gamma) = \frac{L}{A} NZ\sigma_d(\epsilon_\gamma) f(\epsilon_\gamma), \tag{17}$$

where L is the Levinger parameter and $f(\epsilon_\gamma)$ is the Pauli-blocking function. The factor NZ is the total number of neutron-proton pairs inside the nucleus, which is multiplied by a reduction factor L/A to account for the fact that it is only correlated pairs that can be considered to be quasideuterons [40, 41]. In addition, the function $f(\epsilon_\gamma)$ accounts for those excitations of neutron-proton pairs that cannot occur since the Pauli-exclusion principle allows only final particle states which lie above the Fermi level. This effect is particularly important for low photon energies, and Levinger suggested that it can be represented by an exponential Pauli-blocking function [35]

$$f_{Lev}(\epsilon_\gamma) = e^{-D/\epsilon_\gamma}, \tag{18}$$

where D is a constant. Although a theoretical estimate for the Levinger parameter is well known [?], no theoretical derivation for the Pauli-blocking function has been given. In practice, L and D are treated as free parameters to fit the photoabsorption data. The difficulty in separating the effects of the Levinger parameter and the Pauli-blocking function in Eq. (1) has resulted in a substantial ambiguity in the L and D-values used by different groups; they range from $L = 4.9$ and $D = 60$ MeV (Ref. [42]) to $L = 10$ and $D = 80$ MeV (Ref. [43]). We shall describe below how we calculate L and $f(\epsilon_\gamma)$ theoretically.

Our starting point is an expression derived by Levinger [33] for the photoabsorption cross section on a neutron-proton pair, in the absence of Pauli-blocking.

By using effective range theory Levinger was able to relate the photabsorption on a quasideuteron inside the nucleus with relative momentum k, $\sigma_{qd}(k, \epsilon_\gamma)$, to that on a free deuteron, which is known experimentally.

$$\sigma_{qd}(k, \epsilon_\gamma) = \sigma_d(\epsilon_\gamma) \frac{2\pi(1 - \alpha r_0)}{V\alpha} \frac{1}{\alpha^2 + (k/\hbar)^2}, \tag{19}$$

where $k = \frac{1}{2}|\mathbf{k}_\nu - \mathbf{k}_\pi|$ is the initial relative momentum of a neutron-proton pair. $\alpha^{-1} = (\hbar/(2.23m)^{\frac{1}{2}})$ is related to the neutron-proton scattering length [†], m being the nucleon mass, and r_0 is the effective range. The nuclear volume in the above expression is $V = \frac{4}{3}\pi 1.2^3 A$ fm^3.

Following Levinger, we assume that if all the possible final neutron and proton states after photoabsorption are not Pauli-blocked, the photoabsorption cross section on a quasideuteron is given by Eq. (19). However, if the available phase space for the neutron and proton after photoabsorption is reduced by Pauli-blocking, we assume that the quasideuteron photoabsorption cross section is also reduced by the same amount. Thus we suppose that the cross section for photoabsorption is proportional to the available phase space. This is reasonable since Fermi's Golden Rule ought to be applicable as the electromagnetic perturbation is small compared to the nuclear interactions.

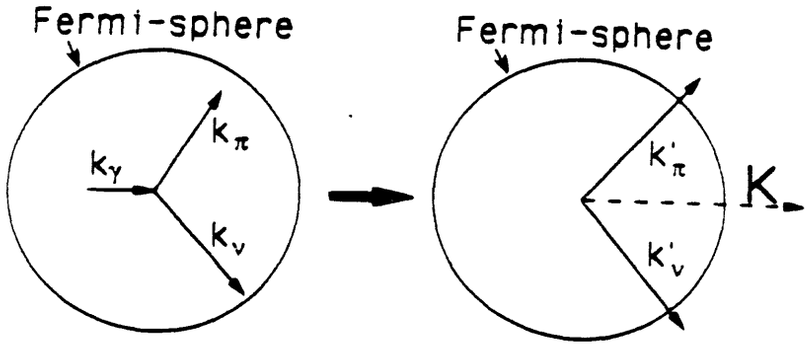

FIG. 5. Absorption of a hard photon by a quasideuteron in the nucleus. The initial linear momenta of the photon, neutron, and proton are $\mathbf{k}_\gamma$, $\mathbf{k}_\nu$, $\mathbf{k}_\pi$ respectively, and the final linear momenta are $\mathbf{k}'_\nu$, $\mathbf{k}'_\pi$. The total momentum is $\mathbf{K}$.

Figure 5 shows, in momentum space, the absorption of a hard photon upon a neutron-proton pair within the nucleus. The initial and final linear momenta, and the corresponding energies, are related by

$$\mathbf{k}_\nu + \mathbf{k}_\pi + \mathbf{k}_\gamma = \mathbf{K} = \mathbf{k}'_\nu + \mathbf{k}'_\pi$$

$$\epsilon_\nu + \epsilon_\pi + \epsilon_\gamma = E = \epsilon'_\nu + \epsilon'_\pi, \tag{20}$$

where primes refer to final states after photoabsorption, and $\mathbf{K}$ and E are the total linear momentum and total energy respectively. If the exclusion principle is obeyed

the vectors $\mathbf{k}'_\nu$ and $\mathbf{k}'_\pi$ must extend beyond the Fermi-sphere as defined by the radius k_F. Considering all accessible final states that are consistent with the above constraints, one obtains the neutron-proton state density which depends on $\mathbf{K}$ and E only. This neutron-proton state density is written as $\rho(2p, E, \mathbf{K})$. The blocking factor $F(\mathbf{k}_\nu, \mathbf{k}_\pi, \mathbf{k}_\gamma)$ can then be expressed as the ratio of this two-particle state density to the one that is obtained when the Pauli exclusion principle is excluded,

$$F(\mathbf{k}_\nu, \mathbf{k}_\pi, \mathbf{k}_\gamma) = \frac{\rho(2p, E, \mathbf{K})}{\rho^{\text{NO PAULI}}(2p, E, \mathbf{K})}, \tag{21}$$

so that the photoabsorption on a particular quasideuteron pair with momenta $\mathbf{k}_\pi$, $\mathbf{k}_\nu$ is $\sigma_{qd}(k, \epsilon_\gamma) \times F(\mathbf{k}_\nu, \mathbf{k}_\pi, \mathbf{k}_\gamma)$ In order to determine the $2p$ state density with linear momentum, a 'two-component' version of Eq. (2) was used. Neutrons and protons are distinguished in this calculation, the neutron and proton single-particle densities in momentum space being given by $\kappa_\nu = N/(\frac{4}{3}\pi k_F^3)$ and $\kappa_\pi = Z/(\frac{4}{3}\pi k_F^3)$. The resulting state density has dimensions ((MeV)$^{-1}$ (MeV/c)$^{-3}$) and is given by

$$\rho(2p, E, \mathbf{K}) =$$

$$\begin{cases} 2\pi m \kappa_\nu \kappa_\pi \sqrt{mE - \frac{K^2}{4}} & \text{if} \begin{cases} mE \geq k_F^2 + k_F K + \frac{1}{2}K^2 \\ \text{or } K \geq 2k_F \text{ and } \frac{1}{4}K^2 \leq mE \leq k_F^2 - k_F K + \frac{1}{2}K^2 \end{cases} \\ 2\pi m \kappa_\nu \kappa_\pi \left[\frac{mE - k_F^2}{K}\right] & \text{if} \begin{cases} K \geq 2k_F \text{ and } k_F^2 - k_F K + \frac{1}{2}K^2 \leq mE \leq k_F^2 + k_F K + \frac{1}{2}K^2 \\ \text{or } K \leq 2k_F \text{ and } mE \leq k_F^2 + k_F K + \frac{1}{2}K^2 \end{cases} \\ 0 & \text{if} \begin{cases} K \leq 2k_F \text{ and } mE \leq k_F^2 \\ \text{or } K \geq 2k_F \text{ and } mE \leq \frac{1}{4}K^2. \end{cases} \end{cases} \tag{22}$$

The two-particle state density that includes all transitions (including those that violate the Pauli principle) can be obtained from the results in Eq. (22) in the limit of $k_F \rightarrow 0$, yielding

$$\rho^{\text{NO PAULI}}(2p, E, \mathbf{K}) = \begin{cases} 2\pi m \kappa_\nu \kappa_\pi \sqrt{mE - \frac{K^2}{4}} & \text{if } mE \geq \frac{1}{4}K^2 \\ 0 \text{ otherwise.} \end{cases} \tag{23}$$

Equations (22) and (23) are used to evaluate the photoabsorption cross section on a specific quasideuteron in the nucleus. The nuclear photoabsorption cross section is then obtained by integrating $\sigma_{qd}(k, \epsilon_\gamma) \times F(\mathbf{k}_\nu, \mathbf{k}_\pi, \mathbf{k}_\gamma)$ over all possible neutron-proton pairs in a Fermi-gas nucleus. Such an integration yields a nuclear photoabsorption cross section of the form (17), with a Levinger parameter of $L = 6.5$ and a Pauli-blocking function as shown in Fig. 6 below. Fig. 6 also shows phenomenological exponential blocking functions with $D = 60$ and $D = 80$ MeV for comparison.

Our Pauli-blocking function has the same general energy dependence as that of Levinger's *ad hoc* exponential function, i.e. at low incident energies it tends to zero and at high energies to unity, as it must, but the exact energy variation is rather

different (see Fig. 6). We note that is not possible to reproduce the steep energy dependence of $f(\epsilon_\gamma)$ which we obtain with a phenomenological exponential function. Since the Pauli-blocking function calculation requires such a large amount of c.p.u. time, we have found a polynomial fit to our results to facilitate future uses of our Pauli-blocking function in nuclear reaction calculations and data evaluations. Our results can be well approximated in the photon energy range 20-140 MeV by the polynomial

$$f(\epsilon_\gamma) = 8.3714 \times 10^{-2} - 9.8343 \times 10^{-3}\epsilon_\gamma + 4.1222 \times 10^{-4}\epsilon_\gamma^2$$

$$-3.4762 \times 10^{-6}\epsilon_\gamma^3 + 9.3537 \times 10^{-9}\epsilon_\gamma^4. \qquad (24)$$

In Fig. 7 we show our calculated quasideuteron contribution to the nuclear photoabsorption cross section compared with data for the nuclei Pb, Ta, Sn and Ce. We also show the tails of the giant dipole resonances (GDR) which may contribute even at these high photon energies. The data as well as the GDR tails are taken from Ref. [36], and the photodisintegration cross section was taken from [44] It is seen that the sum of these two contributions describes the data fairly well. The comparison with data that we obtain seems to be better than that obained with a phenomenological exponential Pauli-blocking function (see, for instance, Leprêtre *et al* [36]. If their quasideuteron component is added to the GDR component they significantly over-estimate the data below a photon energy of 40 MeV).

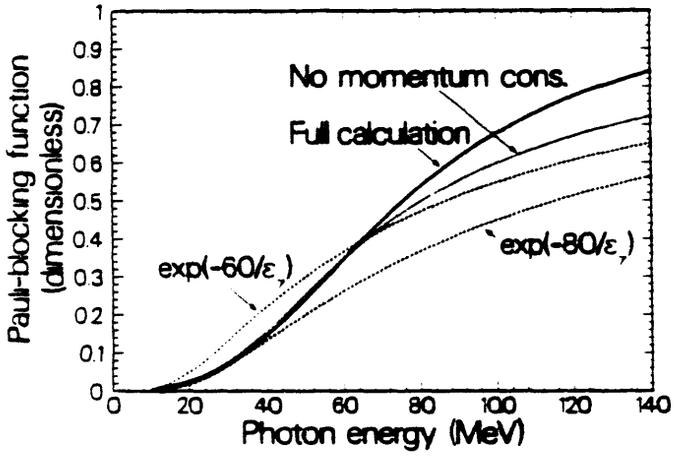

Fig 6

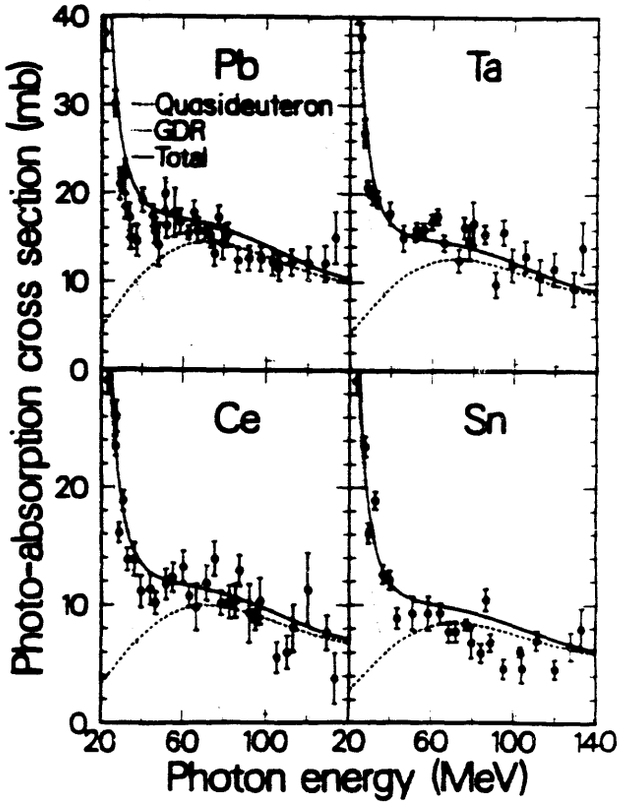

Fig 7.

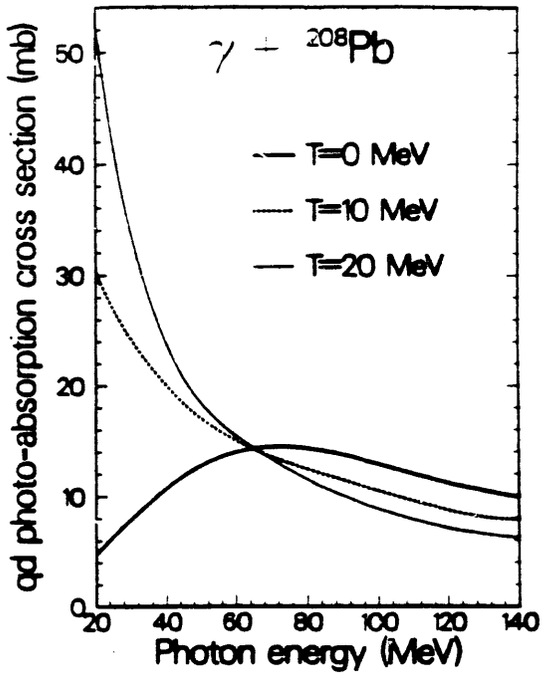

Fig 8

FIG. 6. The calculated quasideuteron component of the nuclear photoabsorption cross section as a function of photon energy is compared with experimental data for Pb, Ta, Sn and Ce. The full curve is the sum of the quasideuteron and GDR contributions. The tails of the GDR as well as experimental data are taken from Ref. [36].

We have also investigated the temperature dependence of the quasideuteron photoabsorption cross section. This is of interest since detailed balance can be applied to determine photon emission rates from hot nuclei produced in heavy-ion collisions via a quasideuteron mechanism [42, 45]. We assumed a Fermi-Dirac distribution of single-particle states and calculated state densities which are a function of energy, linear momentum, and temperature [?]. The photoabsorption cross section was found to be extremely sensitive to temperature, and an example of our results for photobasorption on ^{208}Pb is shown in Fig. 8.

IV. SUMMARY

We have introduced the concept of state densities with linear momentum, and have indicated an exact method for their determination. Our calculational procedure differs from that of Madler and Reif, and can be applied in the determination of state densities of simple particle-hole configurations. Simple analytic expressions can be found for such densities, facilitating their use in nuclear reaction theories. Two different applications for state densities with linear momentum have been presented.

The inclusion of linear momentum effects in an exciton model is able to explain the forward-peaked angular distributions observed in preequilibrium decay, and the angular distributions which they yield are identical to those seen in KK quasifree scattering. We have, therefore, provided a link between exciton model and quasifree scattering descriptions of nuclear reactions, and have provided further justification for the commonly adopted procedure of using a KK scattering kernel in an exciton model. We have also discussed state densities with linear momentum in an equidistant single-particle-state model, and have given expressions which allow angular distributions to be determined (though we also pointed out that the angular distributions would be almost identical to those of KK).

The quasideuteron model of photoabsorption that we have developed is based on phase space arguments and uses state densities with linear momentum. We have presented, for the first time, a theoretical basis for Pauli-blocking effects, and our no-parameter model is able to give a good description of the photoabsorption data for a wide range of nuclei. Our state densities, when generalised to include temperature dependence, were used to determine the quasideuteron photoabsorption cross section on an equilibrated hot nucleus. We found the cross section to be very sensitive to temperature.

These two applications have demonstrated the richness of state densities with linear momentum. They seem to have considerable versatility in their possible applications within nuclear reaction theories. We are presently investigating their application in hard-photon emission reactions and stopped pion-absorption processes.

We would like to thank Drs. M. Blann, P.E. Hodgson, D. Madland, G. Reffo, R. Smith and P.G. Young for helpful discussions, and one of us (M.B.C) acknowledges financial support from an SERC/NATO Fellowship.

REFERENCES

[1] T. E. Ericson, Adv. in Phys. **9**, 425 (1960).

[2] F. C. Williams, Nucl. Phys. **A166**, 231 (1971).

[3] P. Obložinský, Nucl. Phys. **A453**, 127 (1986); E. Betak and J. Dobes, Z. Phys/ **A279**, 319 (1976).

[4] H. Gruppelaar, ECN report ECN-83-064.

[5] C. Kalbach, Phys. Rev. C**30**), 1310 (1984); Los Alamos Report LA-UR-91-2302.

[6] M.B. Chadwick and P. Oblozinsky, to be published in the November 1991 issue of Phys. Rev. C (Rapid Communications).

[7] M.B. Chadwick, P. Obložinský, P.E. Hodgson and G. Reffo, Phys. Rev. C. **44**, 814 (1991).

[8] P. Mädler and R. Reif, Nucl. Phys. **A337**, 445 (1980).

[9] A. Iwamoto, Phys. Rev. C **35**, 984 (1987).

[10] K. Kikuchi and M. Kawai, *Nuclear Matter and Nuclear Reactions*, (North-Holland, Amsterdam, 1968), p. 44; M.L. Goldberger, Phys. Rev. **74**, 1269 (1948).

[11] M. Chadwick and G. Reffo, Phys. Rev. C. **44**, 919 (1991)

[12] H. Feshbach, A. Kerman, and S. Koonin, Ann. Phys. **125**, 429 (1980); R. Bonetti, M.B. Chadwick, P.E. Hodgson, B.V. Carlson, and M.S. Hussein, Physics Reports **202(4)**, 171 (1991).

[13] T. Tamura, T. Udagawa, and H. Lenske, Phys. Rev. C **26**, 379 (1982).

[14] A.J. Koning and J.M. Akkermans, Ann. Phys. **208**, 216 (1991).

[15] A. Marcinkowski, R.W. Finlay, J. Rapaport, P.E. Hodgson, and M.B. Chadwick, Nucl. Phys. **A501**, 1 (1989).

[16] H. Gruppelaar, P. Nagel, and P.E. Hodgson, Riv. Nuovo Cimento **9**, 1 (1986).

[17] M. Blann, Ann. Rev. Nucl. Sci. **25**, 123 (1975).

[18] G. Mantzouranis, D. Agassi, and H.A. Weidenmüller, Phys. Lett. **57B**, 220 (1975); G. Mantzouranis, D. Agassi, and H.A. Weidenmüller, Z. Phys. **A 276**, 145 (1976)

[19] J.M. Akkermans, H. Gruppelaar and G. Reffo, Phys. Rev. C **22**, 73 (1980).

[20] Sun Ziyang, Wang Shunuan, Zhang Jingshang, Zguo Yihong and Han Huiyi, Z. Phys. **A 305**, 61 (1982).

[21] C. Costa, H. Gruppelaar and J.M. Akkermans, Phys. Rev. C **28**, 587 (1983).

[22] M. Blann, W. Scobel and E. Plechaty, Phys. Rev. C **30**, 1493 (1984).

[23] R.D. Smith and M. Bozoian, Phys. Rev. C **39**, 1751 (1989).

[24] H. Machner, Z. Phys. **A 327**, 175 (1987).

[25] E. Gadioli in *Proceedings of the International Conference on Nuclear Reaction Mechanisms*, Saha Institute of Nuclear Physics, Calcutta, Jan. 3-9 (1989), edited by S. Mukherjee (World Scientific, Singapore, 1989), p. 145.

[26] H.C. Chiang and J. Hüfner, Nucl. Phys. **A349**, 466 (1980).

[27] A.L. Fetter and J.D. Walecka, *Quantum Theory of Many-Particle Systems*, (McGraw-Hill, New York, 1971), p. 161.
[28] C. Kalbach, Z. Phys. **A287**, 319 (1978).
[29] C.K. Cline, Nucl. Phys. **A193**, 417 (1972).
* In the recent preequilibrium calculations of F. Cvelbar, E. Betak and J. Merhar (J. Phys. **G17**, 113 (1991)) a value of K=100 MeV^3 in the damping matrix element was adopted. Since our emission rates found using Fermi-gas levels are somewhat smaller than those obtained using equidistant levels, K was increased to 135 MeV^3. The larger rates in our Fermi-gas calculation result from the normalization that we adopted for the single-particle states (Eq. (3)) which result in an underprediction of the density at the Fermi-level.
[30] F.D. Becchetti and G.W. Greenlees, Phys. Rev. **182**, 1190 (1969).
[31] F.E. Bertrand and R.W. Peelle, Phys. Rev. C **8**, 1045 (1973).
[32] P.G. Young and E.D. Arthur, Los Alamos National Laboratory Report LA-6947, Los Alamos National Laboratory (1977).
† Levinger's notation differs from the usual convention. The conventional inverse n-p scattering length is given by $\alpha - \frac{1}{2}\alpha^2 r_0$. Note also that in the literature there seems to be some confusion concerning r_0. It is the effective range, not the nuclear size parameter.
[33] J. S. Levinger, Phys. Rev. **84**, 43 (1951).
[34] J. S. Levinger, *Nuclear Photo-Disintegration* (Oxford University Press, Oxford, 1960), p.97.
[35] J. S. Levinger, Phys. Lett. **82B**, 181 (1979).
[36] A. Leprêtre, H. Beil, R. Bergère, P. Carlos, J. Fagot, A. De Miniac, and A. Veyssière, Nucl. Phys. **A367**, 237 (1981).
[37] R. Bergère, Nuovo Cim. A **76**, 147 (1983).
[38] J. Ahrens, H. Borchert, K.H. Czock, H.B. Eppler, H. Gimm, H. Gundrum, M. Kroning, P. Riehn, G. Sita Ram, A. Zieger and B. Ziegler, Nucl. Phys. **A251**, 479 (1975).
[39] M.L. Terranova, D.A. De Lima and J.D. Pinheiro Filho, Europhys. Lett. **9** (6), 523 (1989).
[40] F. Murgia and P. Quarati, Mod. Phys. Lett. A**4**, 1 (1989).
[41] P. C. Stein, A. C. Odian, A. Wattenberg, and R. Weinstein, Phys. Rev. **119**, 348 (1960).
[42] M. Prakash, P. Braun-Munzinger, J. Stachel, and N. Alamanos, Phys. Rev. C **37**, 1959 (1988).
[43] W. M. Alberico, M. Ericson, and A. Molinari, Ann. Phys. (N. Y.) **154**, 356 (1984).
[44] J. R. Wu and C. C. Chang, Phys. Rev C **16**, 1812 (1977).
[45] N. Herrmann *et al*, Phys. Rev. Lett. **60**, 1630 (1988).

END

DATE FILMED

12/13/91